厚生労働科学研究費補助金（難治性疾患等克服研究事業）
研究分担報告書

レリーワイル症候群の画像診断に関する研究

研究分担者　宮寄治　国立成育医療センター放射線科

研究要旨

レリーワイル症候群（LWS）で最も特徴的な骨変化は、前腕 Madelung 変形である。本研究では、LWS 患者の前腕レントゲン画像解析から、本症の骨変化の発症機序を検討した。

本症では、もっとも初期に橈骨遠位端尺骨側の成長板の不均一な早期閉鎖が生じることが明らかとなった。その後、橈骨、尺骨、月状骨を結ぶ異常な靭帯 (Vickers ligament) が形成される。Vickers ligament 存在下に骨の伸長が生じるため、月状骨の変位と尺骨亜脱臼など、Madelung 変形に典型的な骨変化が生じると推測される。今後、MRI を用いた Vickers ligament の早期同定が可能になれば、その知見は、靭帯切除術という LWS の新たな外科的治療法の開発に結び付く可能性がある。

共同研究者
なし

A．研究目的

レリーワイル症候群 (LWS) は、成長障害と四肢骨の変形を主徴とするまれな先天性骨形成異常症である。患者では、四肢骨変形に起因する疼痛、関節可動域制限が認められる。本症に最も特徴的な所見は、前腕 Madelung 変形である。

本研究班ではこれまでに、本症の初期の画像において、橈骨遠位端尺骨側の不均一な早期融合像が重要であることを見出した。また、変形が進行した状態では、橈骨の湾曲と短縮、月状骨の近位への変位、橈骨と尺骨遠位側の先鋭化等の所見が認められることを明らかとした。

本年度は、新たな患者の画像の解析を行い、これまでの成果をもとに Madelung 変形の発症機序の検討を行った。

B．研究方法

臨床的に LWS と診断された患者の画像データを収集し、本症に特徴的なレントゲン所見について検討した。解析したデータには単純レントゲン、3D-CT が含まれる。

（倫理面への配慮）

本研究の遺伝子解析と患者登録は、国立成育医療研究センター倫理委員会において承認されている。

C．研究結果

1．単純レントゲン像

新たに集積された患者の画像解析を行った。中等度から重度の思春期年齢以降の女性患者 3 名の正面像では、明瞭な Carpal angle 狭小化（通常　118°以上であるが、患者では 100-108°であった。）、橈骨短縮、月状骨の近位への変位を認めた　（図 1）。

側面像では、尺骨の亜脱臼が明瞭に認められた（図 2）。

図 1.　中等度の LWS 成人女性患者のレントゲン像（正面）。
月状骨の近位への変位、Carpal　angle 狭小化、橈骨短縮が認められる。

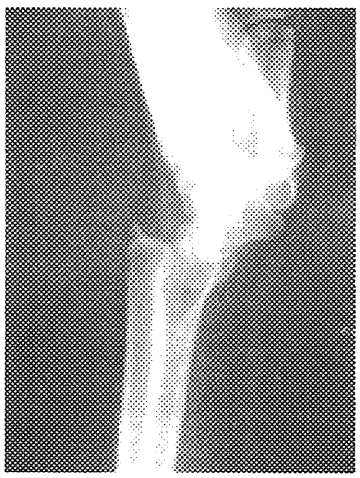

図 2.　上記患者の側面レントゲン像。
尺骨亜脱臼を認める。

2.　3D-CT 解析
単純レントゲンで得られた情報に加え、Vickers ligament の付着部と推測されるわずかな骨変化が観察された　（図 3）。

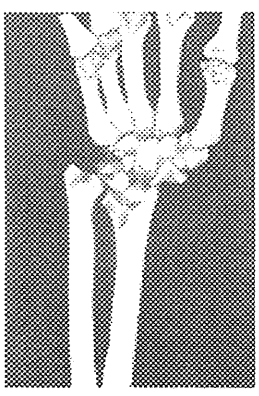

図 3　3D-CT

D．考察

これまでの研究成果から、LWS におけるもっとも早期の変化は、橈骨遠位端尺骨側の成長板の不均一な早期閉鎖であることが示唆される。思春期の成長スパート開始以前このような異常が生じることにより、橈骨内側の成長が障害された状態で骨伸長が進行するため、橈骨、尺骨、月状骨を結ぶ異常な靭帯 Vickers ligament が形成される。Vickers ligament により、月状骨の変位、尺骨亜脱臼など、Madelung 変形の骨変化が生じると推測される。なお、Vickers ligament は、おそらく通常の骨間結合織が引き延ばされることによって形成されるものである。

近年、MRI 検査の解像度の改善に伴い、わずかな結合織の異常をとらえることが可能となった。今後、MRI を用いて Madelung 変形が軽度の小児期において、Vickers ligament の形成を同定することが可能になれば、その成果は Vickers ligament 切除という LWS の新規外科的治療法に結び付くと期待される。

E．結論

画像解析から、LWS の Madelung 変形の重症化には、橈骨、尺骨、月状骨を結ぶ異常な靭帯 Vickers ligament の関与が大きいことが示唆される。Vickers ligament の画像診断は、LWS の新規治療法に結び付く可能性がある。

G．研究発表

1．論文発表

1.　なし

2．学会発表

なし

研究成果の刊行一覧表

研究成果の刊行に関する一覧表

雑誌

発表者氏名	論文タイトル名	発表誌名	巻号	ページ	出版年
Inoue H, Mukai T, Sakamoto Y, Ogata T, et al.	Identification of a novel mutation in the exon 2 splice donor site of the POU1F1/PIT-1 gene in Japanese identical twins with mild combined pituitary hormone deficiency.	*Clin Endocrinol*	76 (1)	78–87	2012
Sugihara S, Ogata T, Kawamura T, Urakami T, et al.	Genetic characteristics on HLA-cass II and class I among Japanese type 1A and type 1B diabetic children and their families.	*Pediatr Diabetes*	13 (1)	33–44	2012
Kagami M, Kato F, Matsubara K, Sato T, Nishimura G, Ogata T	Relative frequency of underlying genetic causes for the development of UPD(14)pat-like phenotype.	*Eur J Hum Genet*	20 (9)	928–932	2012
Oto Y, Obata K, Matsubara K, Ogata T,et al.	Growth hormone secretion and its effect on height in pediatric patients with different genotypes of Prader-Willi syndrome.	*Am J Med Genet A*	158A (6)	1477–1480	2012
Fuke-Sato T, Yamazawa K, Nakabayashi K, Ogata Tet al.	Mosaic upd(7)mat in a patient with Silver-Russell syndrome: correlation between phenotype and mosaic ratio in the body and the placenta.	*Am J Med Genet A*	158A (2)	465–468	2012
Stoppa-Vaucher S, Ayabe T, Paquette J, Ogata T, et al.	46, XY gonadal dysgenesis: new *SRY* point mutation in two siblings with paternal germ line mosaicism.	*Clin Genet*	82 (6)	505–513	2012
Abe Y, Aoki Y, Kuriyama S, Ogata T, et al.	Prevalence and clinical features of Costello syndrome and cardio-facio-cutaneous syndrome in Japan: Findings from a nationwide epidemiological survey.	*Am J Med Genet A*	158A (5)	1083–1094	2012
Koyama Y, Homma K, Fukami M, Ogata T, et al.	Two-step biochemical differential diagnosis of classical 21-hydroxylase deficiency and cytochrome P450 oxidoreductase deficiency in Japanese infants using uUrinary Pregnanetriolone / Tetrahydroxycortisone Ratio and 11β-hydroxyandrosterone by Gas chromatography - mass spectrometry.	*Clin Chem*	58 (4)	741–747	2012
Sekii K, Itoh H, Ogata T,et al.	Deterioration of myocardial tissue Doppler indices in a case of fetal hydrothorax as a promising indication for clinical intervention before the development of nonimmune hydrops fetalis.	*Arch Gynecol Obstet*	286 (4)	1079–1080	2012
Kalfa N, Fukami M, Philibert P, Ogata T, et al.	Screening of *MAMLD1* mutations in 70 Children with 46,XY DSD: Identification and functional analysis of two new mutations.	*PLoS One*	7 (3)	e32505	2012
Qin X-Y, Miyado M, Kojima Y, Ogata T, et al	Identification of novel low-dose bisphenol a targets in human foreskin fibroblast cells derived from hypospadias patients.	*PLoS ONE*	7 (5)	e36711	2012

Sekii K, Ishikawa T, Ogata T, Itoh H, Iwashima S.	Fetal myocardial tissue Doppler indices before birth physiologically change in proportion to body size adjusted for gestational age in low-risk term pregnancies.	*Early Hum Dev*	88 (7)	517–523	2012
Fukami M, Tsuchiya T, Takada S, Ogata T,et al.	Complex genomic rearrangements in the *SOX9* 5' region in a patient with Pierre Robin sequence and hypoplastic left scapula.	*Am J Med Genet A*	158A (7)	1529–1534	2012
Ogata T, Fukami M, Yoshida R, Nagata E, Fujisawa Y, Yoshida A, Yoshimura Y	Haplotype analysis of *ESR2* in Japanese patients with spermatogenic failure.	*J Hum Genet*	57 (7)	449–452	2012
Qin X-Y, Kojima Y, Ogata T,et al.	Association of variants in genes involved in environmental chemical metabolism and risk of cryptorchidism and hypospadias	*J Hum Genet*	57 (7)	434–441	2012
Hiura H, Okae H, Miyauchi N, Ogata T, et al.	Characterization of DNA methylation errors in patients with imprinting disorders conceived by assisted reproduction technologies.	*Hum Reprod*	27 (8)	2541–2548	2012
Nagasaki K, Iida T, Ogata T,et al.	*PRKAR1A* mutation affecting cAMP-mediated G-protein-coupled receptor signaling in a patient with acrodysostosis and hormone resistance.	*J Clin Endocrinol Metab*	97 (9)	E1808–1813	2012
Kagami M, Matsuoka K, Nagai T, Ogata T,et al.	Paternal uniparental disomy 14 and related disorders: placental gene expression analyses and histological examinations.	*Epigenetics*	7 (10)	1142–1150	2012
Moritani M, Yokota I, Tsubouchi K, Ogata T,et al.	Identification of INS and KCNJ11 gene mutations in type 1B diabetes in Japanese children with onset of diabetes before 5 yr of age.	*Pediatr Diabetes*	2012 Sep 10. doi	10.1111/j.1399-5448.2012.00917.x.	[Epub ahead of print]
Suzuki-Suwanai A, Ishii T, Haruna H, Ogata T,et al.	A report of two novel NR5A1 mutation families: possible clinical phenotype of psychiatric symptoms of anxiety and/or depression.	*Clin Endocrinol*		(in press)	
Miyado M, Nakamura M, Miyado K, Ogata T,et al.	*Mamld1* deficiency significantly reduces mRNA expression levels of multiple genes expressed in mouse fetal Leydig cells but permits normal genital and reproductive	*Endocrinology*		(in press)	
Sekii K, Itoh H, Ogata T, Iwashima S	Possible contribution of fetal size and gestational age to myocardial tissue Doppler velocities in preterm fetuses.	*Eur J Obstet Gynecol Reprod Biol*		(in press)	
Nagasaki K, Tsuchuya S, Saitoh A, Ogata T, Fukami M.	Neuromuscular symptoms in a patient with familial pseudohypoparathyroidism type Ib diagnosed by methylation-specific multiplex ligation-dependent probe amplification.	*Endocr J*		(in press)	
Ohishi A, Ueno D, Matsuoka, H, Kawamoto, F Ogata T	Glucose-6-phosphate dehydrogenase deficiency and adrenal hemorrhage in a Filipino neonate with hyperbilirubinemia.	*Am J Perinatol Reports*		(in press)	
Fuke T, Mizuno S, Nagai T, Hasegawa T, Ogata Tet al.	Molecular and clinical studies in 138 Japanese patients with Silver-Russell syndrome.	*PLoS ONE*		(in press)	

Ayabe T, Matsubara K, Ogata T, Ayabe A, Murakami N, Nagai T, Fukami M	Birth seasonality in Prader-Willi syndrome resulting from chromosome 15 microdeletion.	*Am J Med Genet A*		(in press)	
Fukami M, Shozu M, Ogata T	Molecular bases and phenotypic determinants of aromatase excess syndrome.	*Int J Endocrinol*	2012	584807	2012
Ogata T, Sano S, Nagata E, kato F, Fumaki M	*MAMLD1* and 46,XY disorders of sex development.	*Semi Reprod Med*	30 (5)	410–416	2012
Fukami M, Homma K, Hasegawa T, Ogata T	Backdoor pathway for dihydrotestosterone biosynthesis: implications for normal and abnormal human sex development.	*Dev Dyn*		10.1002/dvdy.23892	[Epub ahead of print]
Takagi1 M, Ishii T, Inokuchi M, Amano N, Narumi S, Asakura Y, Muroya K, Hasegawa Y, Adachi M, Hasegawa T.	Gradual Loss of ACTH Due to a Novel Mutation in LHX4: Comprehensive Mutation Screening in Japanese Patients with Congenital Hypopituitarism.	*PLOS ONE*	7 (9)	e46008	2012
Takagi T, Seki A, Matsumoto H, Morisawa Y, Kusakabe H, Takayama S	A radiographic method for evaluation of the index-hypoplastic thumb angle.	*J Hand Surg Am.*	37(11)	2320-2324	2012
佐々木康介, 関敦仁, 宮崎馨, 高木岳彦, 日下部浩, 高山真一郎, 松本守雄	Morquio 症候群に対する整形外科手術	日小整会誌	21(1)	136-140	2012
中村千恵子, 高山真一郎, 関敦仁, 日下部浩, 福岡昌利, 谷渕綾乃	VATER association における橈側列異常の特徴について	日小整会誌	21(2)	345-349	2012
関敦仁	上肢の先天異常	*MB Orthop*	25(9)	17-28	2012
関敦仁	骨軟骨異形成症	小児内科	44 増刊号	818-819	2012
関敦仁, 宮崎馨, 高山真一郎	小児の手指にみられる軟骨性腫瘍類似疾患	整・災外	55	503-511	2012

研究成果の刊行物・別刷り

Hindawi Publishing Corporation
International Journal of Endocrinology
Volume 2012, Article ID 584807, 8 pages
doi:10.1155/2012/584807

Review Article

Molecular Bases and Phenotypic Determinants of Aromatase Excess Syndrome

Maki Fukami,[1] Makio Shozu,[2] and Tsutomu Ogata[1,3]

[1] *Department of Molecular Endocrinology, National Research Institute for Child Health and Development, 2-10-1 Ohkura, Setagaya, Tokyo 157-8535, Japan*
[2] *Department of Reproductive Medicine, Graduate School of Medicine, Chiba University, 1-8-1 Inohana, Chuo-ku, Chiba City 206-8670, Japan*
[3] *Department of Pediatrics, Hamamatsu University School of Medicine, 1-20-1 Handayama, Higashi-ku, Shizuoka, Hamamatsu 431-3192, Japan*

Correspondence should be addressed to Maki Fukami, mfukami@nch.go.jp

Received 9 July 2011; Revised 22 September 2011; Accepted 2 October 2011

Academic Editor: Rodolfo Rey

Aromatase excess syndrome (AEXS) is a rare autosomal dominant disorder characterized by gynecomastia. This condition is caused by overexpression of *CYP19A1* encoding aromatase, and three types of cryptic genomic rearrangement around *CYP19A1*, that is, duplications, deletions, and inversions, have been identified in AEXS. Duplications appear to have caused *CYP19A1* overexpression because of an increased number of physiological promoters, whereas deletions and inversions would have induced wide *CYP19A1* expression due to the formation of chimeric genes consisting of a noncoding exon(s) of a neighboring gene and *CYP19A1* coding exons. Genotype-phenotype analysis implies that phenotypic severity of AEXS is primarily determined by the expression pattern of *CYP19A1* and the chimeric genes and by the structural property of the fused exons with a promoter function (i.e., the presence or the absence of a natural translation start codon). These results provide novel information about molecular mechanisms of human genetic disorders and biological function of estrogens.

1. Introduction

Aromatase encoded by *CYP19A1* is a cytochrome P450 enzyme that plays a key role in estrogen biosynthesis [1]. It catalyzes the conversion of Δ^4-androstendione into estrone (E_1) and that of testosterone (T) into estradiol (E_2) in the placenta and ovary as well as in other tissues such as the fat, skin, bone, and brain [1].

Overexpression of *CYP19A1* causes a rare autosomal dominant disorder referred to as aromatase excess syndrome (AEXS, OMIM no. 139300) [2–8]. AEXS is characterized by pre- or peripubertal onset gynecomastia, gonadal dysfunction, advanced bone age from childhood to pubertal period, and short adult height in affected males [2–8]. In particular, gynecomastia is a salient feature in AEXS, and, therefore, this condition is also known as hereditary gynecomastia or familial gynecomastia [5]. Affected females may also show several clinical features such as macromastia, precocious puberty, irregular menses, and short adult height [5, 6, 8].

Recently, three types of cryptic genomic rearrangements around *CYP19A1* have been identified in 23 male patients with AEXS [2–4]. The results provide useful implications not only for the clarification of underlying mechanisms but also for the identification of phenotypic determinants. Here, we review the current knowledge about AEXS.

2. The Aromatase Gene (*CYP19A1*)

CYP19A1 encoding aromatase is located on 15q21.2 adjacent to *DMXL2* and *GLDN* (Figure 1) [3, 9]. It spans ~123 kb and consists of at least 11 noncoding exons 1 and nine coding exons 2–10 [9–12]. Each exon 1 is accompanied by a tissue-specific promoter and is spliced alternatively onto a common splice acceptor site at exon 2, although some transcripts are known to contain two of the exons 1 probably due to a splice error [9–11]. Transcription of *CYP19A1* appears to be tightly regulated by alternative usage of the multiple

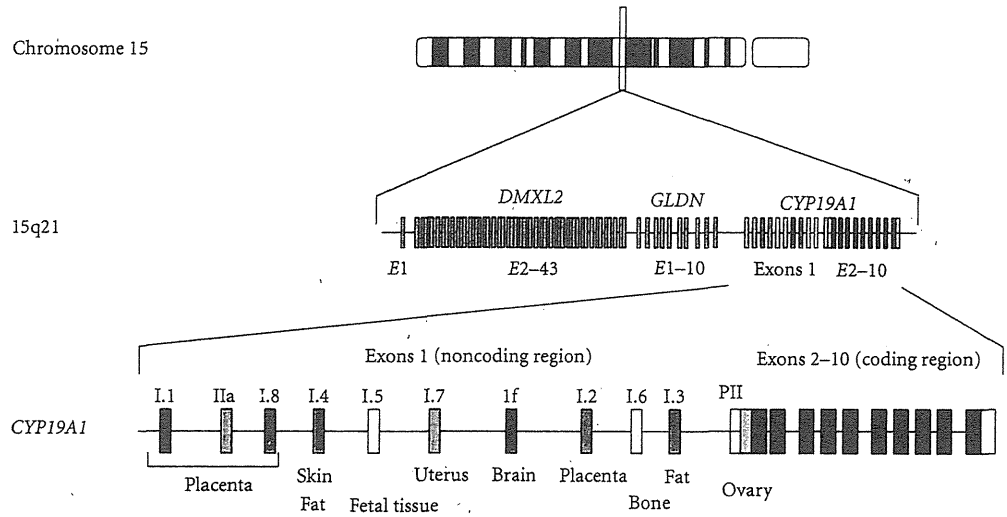

FIGURE 1: Simplified schematic representation indicating the genomic structure of *CYP19A1*. *CYP19A1* is located on 15q21.2 adjacent to *DMXL2* and *GLDN* and consists of at least 11 noncoding exons 1 and nine coding exons 2–10 [9, 10]. Each exon 1 is accompanied by a tissue-specific promoter and is spliced alternatively onto a common splice acceptor site at exon 2 [9–13].

promoters [9–13]. Actually, *CYP19A1* is strongly expressed in the placenta and moderately expressed in the ovary, whereas it is only weakly expressed in a rather limited number of tissues including skin, fat, and hypothalamus [4, 13]. Of the 11 noncoding exons 1, exon I.4 seems to play a critical role in the regulation of estrogen biosynthesis in males, because this exon contains the major promoter for extragonadal tissues [9, 10].

3. Molecular Bases of AEXS

A family with dominantly transmitted gynecomastia of prepubertal onset was first described in 1962 by Wallach and Garcia [14]. After this initial report, several cases have been described [5–8, 15]. Laboratory examinations of the affected males revealed markedly elevated serum estrogen values and estrogen/androgen ratios and significantly increased aromatase activity in fibroblasts and lymphocytes [5–8, 15]. Linkage analyses in two families indicated a close association between *CYP19A1*-flanking polymorphic markers and the disease phenotype [5, 6]. Thus, the condition was assumed to be caused by gain-of-function mutations of *CYP19A1*, and, therefore, the name of AEXS was coined for this condition [7, 8]. However, since direct sequencing and Southern blotting analysis failed to detect mutations or copy number abnormalities in the coding region of *CYP19A1* [5, 6], the molecular basis of this entity remained elusive until recently.

In 2003, Shozu et al. reported a father-son pair and a sporadic case with AEXS in whom they identified heterozygous chromosomal inversions of the chromosome 15 [2]. Subsequently, Demura et al. performed detailed molecular studies for these cases and additional two cases and characterized four types of inversions affecting the 5′ region of *CYP19A1* [3]. Each inversion has resulted in the formation of a chimeric gene consisting of *CYP19A1* coding exons and exon 1 of the widely expressed neighboring genes, that is, *CGNL1*, *TMOD3*, *MAPK6*, and *TLN2*. These data imply that overexpression of *CYP19A1* in the inversion-positive cases are caused by cryptic usage of constitutively active promoters. Consistent with this, *in silico* analysis revealed the presence of promoter-compatible sequences around exon 1 of *CGN1*, *TMOD3*, and *MAPK6* in multiple cell types, although such sequences remain to be identified for noncoding exons of *TLN2* [4].

We recently studied 18 males from six families with AEXS (families A–F) and identified three types of heterozygous cryptic genomic rearrangements in the upstream region of the *CYP19A1* coding exons (Figure 2) [4]. In families A and B, we identified the same 79,156 bp tandem duplication encompassing seven of the 11 noncoding exons 1 of *CYP19A1*. Notably, this duplication includes exon I.4 that functions as a major promoter for extragonadal tissues such as fat and skin; therefore, *CYP19A1* overexpression in these families would be explained by increasing the number of this promoter. Indeed, RT-PCR analysis detected a splice variant consisting of exon I.4 at the 5′ side and exon I.8 at the 3′ side in lymphoblastoid cell lines and skin fibroblasts of the patients, indicating that the duplicated exon I.4 at the distal nonphysiological position actually functions as transcription start sites. In family C, we identified a 211,631 bp deletion affecting exons 2–43 of *DMXL2* and exons 5–10 of *GLDN*. This deletion appears to have caused *CYP19A1* overexpression because of cryptic usage of *DMXL2* exon 1 as an extra transcription start site for *CYP19A1*. Indeed, RT-PCR revealed the presence of chimeric mRNA clones consisting of *DMXL2* exon 1 and *CYP19A1* exon 2, supporting the notion that aberrant splicing has occurred between these two exons. Such *DMXL2*/*CYP19A1* chimeric mRNA accounted for 2–5% of *CYP19A1*-containing transcripts from skin fibroblasts. In families D–F, we identified

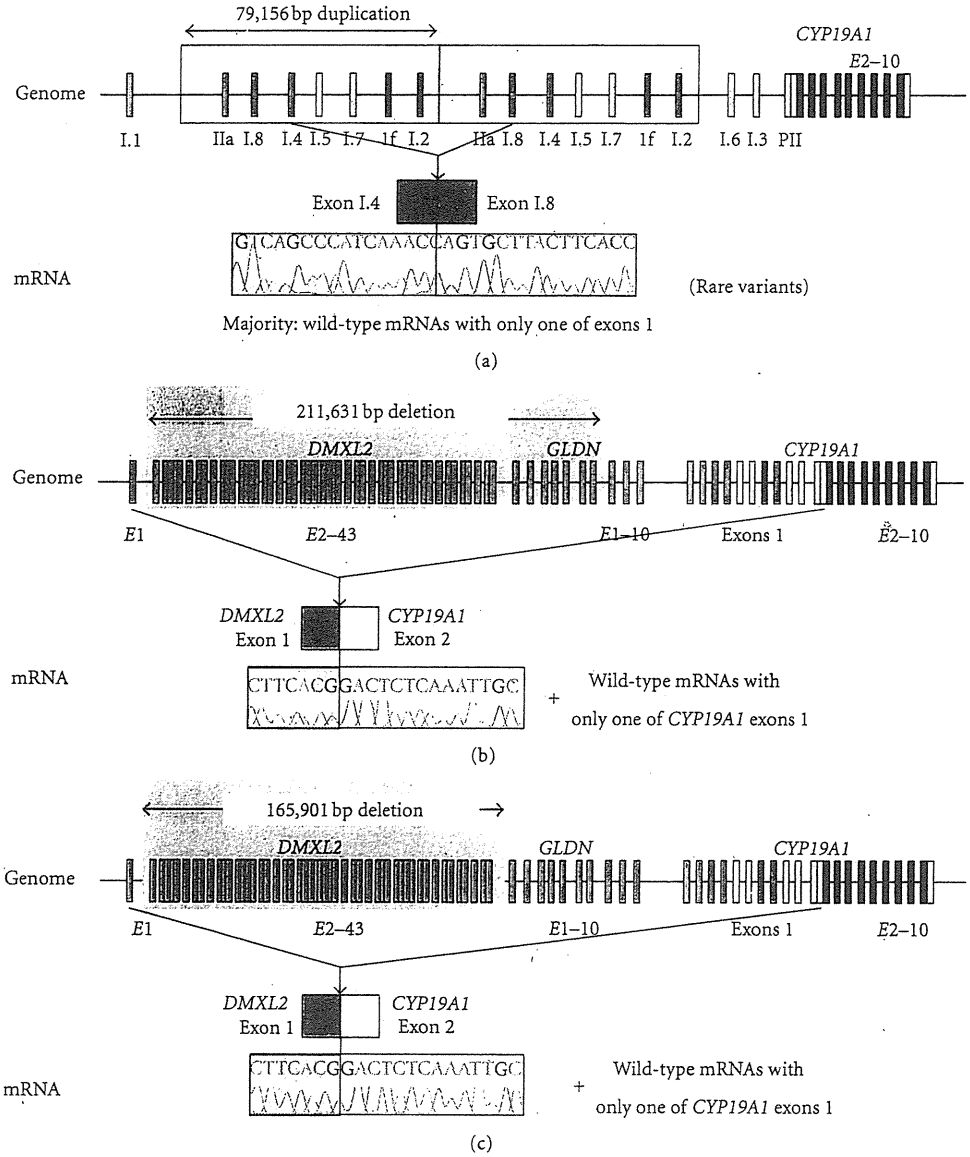

FIGURE 2: Schematic representation of duplications and deletions identified in patients with AEXS. (a) the tandem duplication of families A and B [4]. Genome: the duplication (yellow boxes) includes seven of the 11 noncoding exons 1 of *CYP19A1*. mRNA: the sequence of a rare transcript is shown. The 3′-end of exon I.4 is connected with the 5′-end of exon I.8. (b) The deletion of family C [4]. Genome: the deletion (a gray area) includes exons 2–43 of *DMXL2* and exons 5–10 of *GLDN*. mRNA: The sequence of a rare chimeric gene transcript is shown. *DMXL2* exon 1 consisting of a noncoding region and a coding region is spliced onto the common acceptor site of *CYP19A1* exon 2. (c) The deletion of families D–F [4]. Genome: the deletion (a gray area) includes exons 2–43 of *DMXL2*. mRNA: the sequence of a rare chimeric gene transcript is delineated. The mRNA structure is the same as that detected in family C.

an identical 165,901 bp deletion including exons 2–43 of *DMXL2*. RT-PCR identified the same chimeric mRNA as that detected in family C.

Collectively, three types of genomic rearrangements on 15q21 have been identified in AEXS to date, namely, inversion type (four subtypes), duplication type, and deletion type (two subtypes) (Figure 3(a)) [2–4]. In this regard, sequence analyses for the breakpoints have indicated that (1) inversion types are formed by a repeat sequence-mediated nonallelic intrachromosomal or interchromosomal recombination or by a replication-based mechanism of fork stalling and template switching (FoSTeS) that occurs in the absence of repeat sequences and is often associated with microhomology [16], (2) duplication type is generated by FoSTeS, and (3) deletions are produced by nonhomologous end joining that takes place between nonhomologous sequences and is frequently accompanied by an insertion of a short segment at the fusion point or by a nonallelic recombination [16].

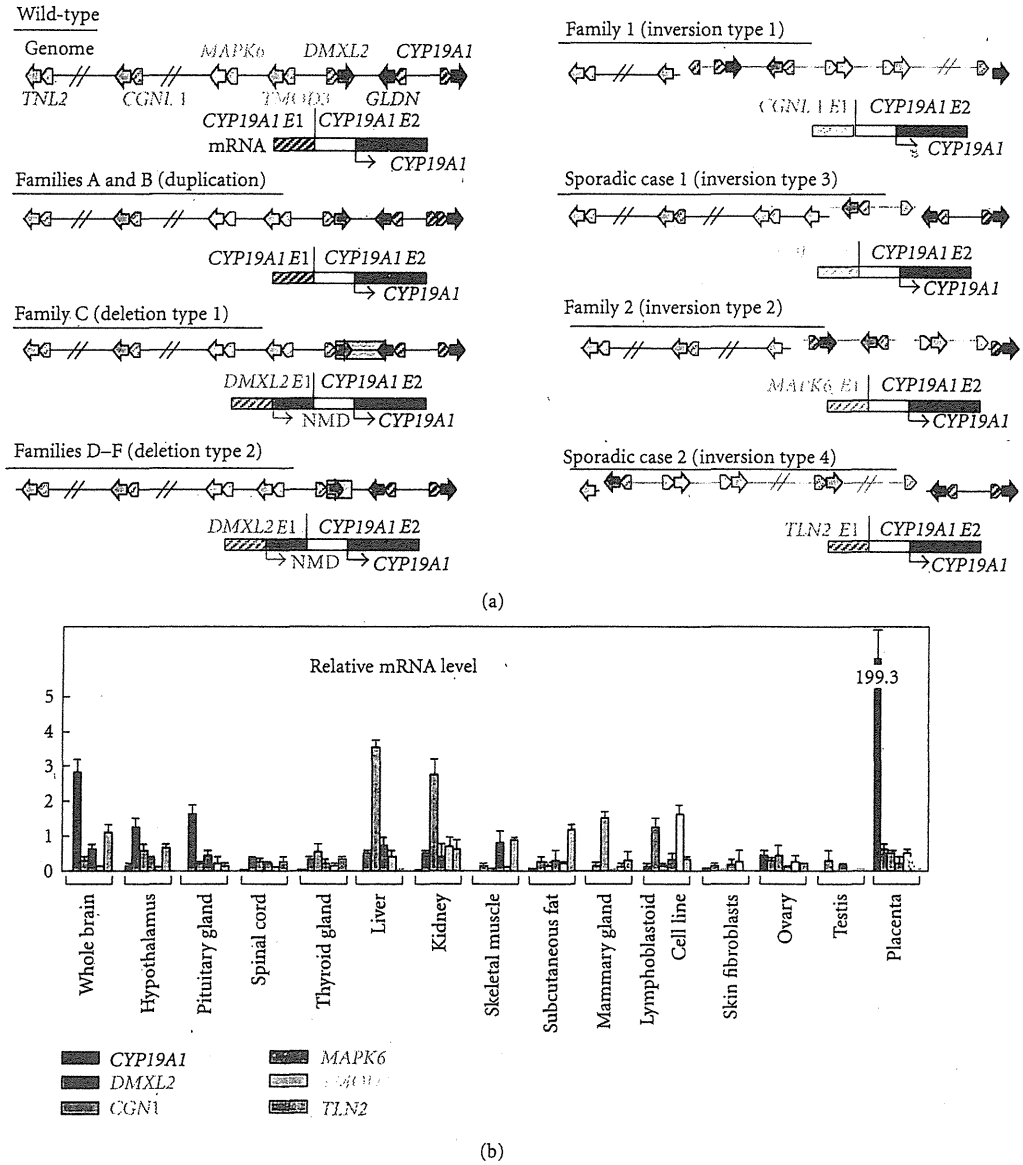

FIGURE 3: Structural and functional properties of the fused exons. (a) Schematic representation of the rearranged genome and mRNA structures. The white and the black boxes of *CYP19A1* exon 2 show untranslated region and coding region, respectively. For genome, the striped and the painted arrows indicate noncoding and coding exons, respectively (5′ → 3′). The inverted genomic regions are delineated in blue lines. For mRNA, colored striped boxes represent noncoding regions of each gene. The *DMXL2-CYP19A1* chimeric mRNA has two translation initiation codons and therefore is destined to produce not only *CYP19A1* protein but also a 47 amino acid protein which is predicted to undergo nonsense-mediated mRNA decay (NMD). The deletion and the inversion types are associated with heterozygous impairment of neighboring genes (deletion or disconnection between noncoding exon(s) and the following coding exons). The inversion subtype 1 is accompanied by inversion of eight of the 11 *CYP19A1* exons 1, and the inversion subtype 2 is associated with inversion of the placenta-specific *CYP19A1* exon I.1. (b) Expression patterns of *CYP19A1* and the five neighboring genes involved in the chimeric gene formation [4]. Relative mRNA levels against *TBP* in normal human tissues are shown.

Thus, it appears that genomic sequence around *CYP19A1* harbors particular motifs that are vulnerable to replication- and recombination-mediated errors. The results provide novel mechanisms of gain-of-function mutations leading to human diseases.

4. Clinical Features of AEXS

To date, a total of 23 male cases from 10 families have been reported to have molecularly confirmed AEXS (Table 1, Figure 3(a)) [2–4]. They exhibited pre- or peripubertal onset

Table 1: Summary of clinical studies in male patients with aromatase excess syndrome (modified from [4]).

(a)

Family			Family A			Family B		Family C				Family D			Family E	
Mutation types			Duplication			Duplication		Deletion				Deletion			Deletion	
The promoter involved in *CYP19A1* overexpression			*CYP19A1*			*CYP19A1*		*CYP19A1*				*DMXL2*			*DMXL2*	
Case		Case 1	Case 2		Case 3		Case 4	Case 5		Case 6		Case 7	Case 8		Case 9		Case 10	
Age at examination (year)		66	15		20		15	15		13		42	9		12		13	
<Phenotypic findings>																		
Gynecomastia (tanner breast stage)		**2**	**2**		**2**		**3**	**4**		**4**		**4**	**3**		**4**		**4**	
Onset of gynecomastia (year)		**13**	**13**		**10**		**11**	**12**		**11**		**11**	**7**		**9**		**10**	
Mastectomy (year)		No	**Yes (15)**		No		**Yes (15)**	**Yes (15)**		**Yes (13)**		No	No		**Yes (12)**		**Yes (13)**	
Testis (ml)		N.E.	**12**		**12**		**12**	**12**		12		N.E.	3		12		20	
Pubic hair (tanner stage)		N.E.	2-3		4		5	4		3		N.E.	1		3		4	
Facial hair		Normal	Scarce		**Scarce**		Normal	Absent		Absent		N.E.	Absent		Absent		Absent	
Height (SDS)[a]		−1.2	−0.3		+0.4		+0.8	−2.0		−1.0		−1.6	**+2.7**		±0		+1.8	
Bone age (year)[b]		N.E.	N.E.		N.E.		16.0	16.0		13.5		N.E.	**13.0**		**15.0**		**17.0**	
Fertility (spermatogenesis)		Yes	?		(Yes)[h]		?	?		?		Yes	?		?		?	
<Endocrine findings>[c]		B	B	S	B	S	B S	B	S	B	S	B	B	S	B	S	B	S
<At Dx>	Stimulus																	
LH (mIU/mL)	GnRH[e]	3.8	2.3	**14.3**	2.1	**17.0**	2.4 29.4	1.9	40.6	1.8	69.2		1.1	11.5	**0.6**	39.5	6.7	14.8
LH (mIU/mL)	GnRH (after priming)[f]		1.8	**9.5**	**1.3**	**10.7**												
FSH (mIU/mL)	GnRH[e]	**1.7**	**3.1**	**5.3**	**<0.5**	**1.2**	**0.9 2.4**	**1.4**	**4.2**	**2.0**	**7.8**		**3.2**	**6.6**	**0.6**	**2.9**	**0.7**	**1.0**
FSH (mIU/mL)	GnRH (after priming)[f]		**2.6**	**3.2**	**<0.5**	**0.9**												
Prolactin (ng/ml)			4.3		5.3			8.2		9.1			11.3		18.8			
Δ^4A (ng/mL)		**0.5**			**1.1**		**1.2**					**0.6**			**0.7**		**2.4**	2.9
T (ng/mL)	hCG[g]	2.9	**1.6**		**2.2**		4.0	**2.6**	7.2	**1.4**	7.9		**0.6**	3.6	**2.4**		3.2	9.7
DHT (ng/mL)		0.4			0.2												0.4	1.2
Inhibin B (pg/mL)		**61.6**			**74.6**		**83.5**	**75.2**										
E_1 (pg/mL)		157			120		124					57			63		53	
E_2 (pg/mL)		29	15		22		59	56		38		24	19		25		58	
E_2/T ratio ($\times 10^3$)		10.0	9.4		10.0		14.8	21.5		27.1			31.7		10.4		18.1	

(b)

Family		Family F								Family G		Family H		Sporadic	
Mutation types		Deletion								Inversion		Inversion		Inversion	
The promoter involved in *CYP19A1* overexpression		*DMXL2*								*CGNL1*		*MAPK6*		*TMOD3*	*TLN2*
Case		Case 11	Case 12	Case 13	Case 14	Case 15	Case 16	Case 17	Case 18	Case 19	Case 20	Case 21[j]		Case 22	Case 23
Age at examination (year)		69	35	44	45	9	8	13	10	35	7	13		17	36
<Phenotypic findings>															
Gynecomastia (tanner breast stage)		Yes[i]	Yes[i]	Yes[i]	Yes[i]	**2**	**3**	**3**	**3**	**Yes**	**3**	**5**		N.E.	**Yes**
Onset of gynecomastia (year)		?	?	?	?	**8**	**8**	**11**	**10**	**5**	**5**	**8**		**7**	?
Mastectomy (year)		Yes[i]	Yes[i]	Yes[i]	Yes[i]	No	No	**Yes (?)**	**Yes (?)**	**Yes (16)**	No	**Yes (?)**		**Yes (?)**	**Yes (19)**
Testis (ml)		N.E.	N.E.	N.E.	N.E.	2	1.5	**2**	2	N.E.	N.E.	N.E.		Normal	N.E.
Pubic hair (tanner stage)		N.E.	N.E.	N.E.	N.E.	1	1	2	1	Normal	1	**2-3** (at 21.0)		N.E.	N.E.
Facial hair		N.E.	N.E.	N.E.	N.E.	Absent	Absent	Absent	Absent	**Absent**	Absent	N.E.		**Scarce**	N.E.
Height (SDS)[a]		N.E.	~ −1.5	~ −1.5	~ −1.5	+1.4	N.E.	**+2.0**	**+2.4**	**Short**	**>+2.5**	−1.6 (at 21.0)		**Short**	N.E.
Bone age (year)[b]		N.E.	N.E.	N.E.	N.E.	**12.5**	**13.0**	**15.0**	**14.5 (at 12.5)**	N.E.	**13.0 (at 5.5)**	**17.0**		N.E.	N.E.
Fertility (spermatogenesis)		Yes	Yes	Yes	Yes	?	?	?	?	Yes	?	?		?	?
<Endocrine findings>[c]		B	B	B	B	B	B	B S	B	B	B	B S		B	
<At Dx>	Stimulus														
LH (mIU/mL)	GnRH[e]	**0.2**	3.5	1.7	3.0	0.2	<0.1	2.6 6.3	1.5	1.7	0.1	2.6	**10.0**	4.3	
LH (mIU/mL)	GnRH (after priming)[f]														
FSH (mIU/mL)	GnRH[e]	**1.4**	**2.3**	**0.8**	**0.8**	1.4	0.5	**0.8** **1.2**	**1.2**	**1.5**	0.3	**<0.1**	**<0.1**	**2.7**	
FSH (mIU/mL)	GnRH (after priming)[f]														
Prolactin (ng/ml)															
Δ^4A (ng/mL)		1.4	**0.4**	1.7	**0.5**	0.3	<0.3	**0.9** 1.5	1.3	**0.8**	0.3	2.4	**0.9**		
T (ng/mL)	hCG[g]	**2.6**	**2.5**	**2.1**	**2.5**	<0.1	<0.1	**2.7** 9.2	**2.7**	3.2	<0.1	**1.2**	3.8	**2.3**	
DHT (ng/mL)												0.2	0.5		
Inhibin B (pg/mL)															
E_1 (pg/mL)		32	34	59	34	26	41	77	86	903	119	544		556	
E_2 (pg/mL)		10	19	24	31	11	7	25	40	223	15	178		392	
E_2/T ratio ($\times 10^3$)		3.8	7.6	11.4	12.4			9.3	14.8	69.6		148.3		170.4	

SDS: standard deviation score; Dx: diagnosis; Tx: therapy; LH: luteinizing hormone; FSH: follicle stimulating hormone; Δ^4A: androstenedione; T: testosterone; DHT: dihydrotestosterone; E_1: estrone; E_2: estradiol; GnRH: gonadotropin-releasing hormone; hCG: human chorionic gonadotropin; N.E.: not examined; B: basal; and S: stimulated.

Abnormal clinical findings are boldfaced.

Abnormally low hormone values are boldfaced, and abnormally high hormone values are underlined.

[a]Evaluated by age- and ethnicity-matched growth references; heights ≥+2.0 SD or below ≤ −2.0 SD were regarded as abnormal.

[b]Assessed by the Tanner-Whitehouse 2 method standardized for Japanese or by the Greulich-Pyle method for Caucasians; bone age was assessed as advanced when it was accelerated a year or more.

[c]Evaluated by age-matched male reference data, except for inhibin B and E_1 that have been compared with data from 19 adult males.

[d]Treated with aromatase inhibitors (anastrozole).

[e]GnRH 100 μg/m^2 (max. 100 μg) bolus i.v.; blood sampling at 0, 30, 60, 90, and 120 minutes.

[f]GnRH test after priming with GnRH 100 μg i.m. for 5 consecutive days.

[g]hCG 3000 IU/m^2 (max 5000 IU) i.m. for 3 consecutive days; blood sampling on days 1 and 4.

[h]Although Case 3 has not yet fathered a child, he has normal spermatogenesis with semen volume of 2.5 ml (reference value: >2 ml), sperm count of 105 × 10^6/ml (>20 × 10^6/ml), total sperm count of 262.5 × 10^6 (>40 × 10^6), motile cells of 70% (>50%), and normal morphological sperms 77% (>30%).

[i]These four patients allegedly had gynecomastia that required mastectomy (age unknown).

[j]The sister has macromastia, large uterus, and irregular menses; the parental phenotype has not been described.

The conversion factor to the SI unit: LH 1.0 (IU/L), FSH 1.0 (IU/L), E_1 3.699 (pmol/L), E_2 3.671 (pmol/L), Δ^4A 3.492 (nmol/L), and T 3.467 (nmol/L).

gynecomastia, small testes with fairly preserved masculinization, obvious or relative tall stature in childhood and grossly normal or apparent short stature in adulthood, and age-appropriate or variably advanced bone ages. Blood endocrine studies revealed markedly elevated E_1 values and E_2/T ratios in all cases examined and normal or variably elevated E_2 values. In addition, Δ^4-androstenedione, T, and dihydrotestosterone values were low or normal, and human chorionic gonadotropin (hCG) test indicated normal T responses. Notably, LH values were grossly normal at the baseline and variably responded to GnRH stimulation, whereas FSH values were low at the baseline and poorly responded to GnRH stimulation even after preceding GnRH priming, in all cases examined.

The severity of such clinical phenotypes is primarily dependent on the underlying mechanisms (Table 1). They are obviously mild in the duplication type, moderate in the deletion type, and severe in the inversion type, except for serum FSH values that remain suppressed irrespective of the underlying mechanisms. Likewise, gynecomastia has been reported to be ameliorated with 1 mg/day of aromatase inhibitor (anastrozole) in the duplication and the deletion types and with 2–4 mg/day of anastrozole in the inversion type [4].

5. Expression Pattern of *CYP19A1* and the Chimeric Genes as One Phenotypic Determinant

Phenotypic severity is much milder in the duplication type than in the deletion and the inversion types. This would be explained by the tissue expression pattern of *CYP19A1* and the chimeric genes. Indeed, RT-PCR analysis using normal human tissue samples revealed that *CYP19A1* is expressed only in a limited number of tissues such as placenta, ovary, skin, and fat, while the five genes involved in the formation of chimeric genes are widely expressed with some degree of variation (Figure 3(b)). Therefore, it is likely that the duplication types would simply increase *CYP19A1* transcription in native *CYP19A1*-expressing tissues, whereas the deletion and the inversion types lead to *CYP19A1* overexpression in a range of tissues, because expression patterns of chimeric genes are predicted to follow those of the original genes. Furthermore, it is also likely that the native *CYP19A1* promoter is subject to negative feedback by elevated estrogens [17], whereas such negative feedback effect by estrogen is weak or even absent for the chimeric genes in the deletion and the inversion types.

6. Structural Property of the Fused Exons as Another Phenotypic Determinant

Phenotypic severity is also milder in the deletion type than in the inversion types, despite a similar wide expression pattern of genes involved in the chimeric gene formation (Table 1, Figure 3(b)). In this context, it is noteworthy that a translation start codon and a following coding region are present on exon 1 of *DMXL2* of the deletion type but not on exons 1 of the chimeric genes of the inversion types (Figure 3(a)). Thus, it is likely that *DMXL2/CYP19A1* chimeric mRNAs transcribed by the *DMXL2* promoter preferentially recognize the natural start codon on *DMXL2* exon 1 and undergo nonsense-mediated mRNA decay and that rather exceptional chimeric mRNAs, which recognize the start codon on *CYP19A1* exon 2, are transcribed into CYP19A1 protein. By contrast, such a phenomenon would not be postulated for the inversion-mediated chimeric mRNAs. Consistent with this, it has been shown that the *DMXL2/CYP19A1* chimeric mRNA is present only in 2–5% of *CYP19A1*-containing transcripts from skin fibroblasts, whereas the *CGNL1/CYP19A1* chimeric mRNA and the *TMOD3/CYP19A1* chimeric mRNA account for 89–100% and 80% of transcripts from skin fibroblasts, respectively [2, 4].

In addition, the genomic structure caused by the rearrangements would affect efficiency of splicing between noncoding exon(s) of neighboring genes and *CYP19A1* exon 2. For example, in the inversion subtype 1, the physical distance between *CGNL1* exon 1 and *CYP19A1* exon 2 is short, and, while a splice competition may be possible between exon 1 of neighboring genes and original *CYP19A1* exons 1, eight of 11 *CYP19A1* exons 1 including exon I.4 have been disconnected from *CYP19A1* coding exons by inversion (Figure 3(a)). This may also enhance the splicing efficiency between *CGNL1* exon 1 and *CYP19A1* exon 2 and thereby lead to relatively severe overexpression of the *CGNL1-CYP19A1* chimeric gene, although this hypothesis would not be applicable for other chimeric genes.

7. Implication for the Hypothalamus-Pituitary-Gonadal Axis Function

It is notable that a similar degree of FSH-dominant hypogonadotropic hypogonadism is observed in the three types, although E_1 and E_2 values and E_2/T ratios are much higher in the inversion type than in the duplication and deletion types (Table 1). In particular, FSH was severely suppressed even after GnRH priming in the duplication type [4]. This implies that a relatively mild excess of circulatory estrogens can exert a strong negative feedback effect on FSH secretion primarily at the pituitary. This would be consistent with the results of animal studies that show strong inhibitory effect of E_2 on transcription of FSH beta-subunit gene in the pituitary cells and almost negligible effect on synthesis of LH beta-subunit and secretion of LH [18, 19]. In this regard, while T responses to hCG stimulation are normal in the duplication and the deletion types and somewhat low in the inversion type, this would be consistent with fairly preserved LH secretion in the three types and markedly increased estrogen values in the inversion type. In addition, whereas fertility and spermatogenesis are normally preserved in the three types, this would be explained by the FSH-dominant hypogonadotropic hypogonadism, because FSH plays only a minor role in male fertility (spermatogenesis) [20].

8. Conclusions

Current studies argue that AEXS is caused by overexpression of *CYP19A1* due to three different types of cryptic genomic rearrangements including duplications, deletions, and inversions. It seems that transcriptional activity and structural property of the fused promoter constitutes the underlying factor for the clinical variability in most features of AEXS except for FSH-dominant hypogonadotropic hypogonadism. Thus, AEXS represents a novel model for gain-of-function mutation leading to human genetic disorders.

References

[1] S. Bhasin, "Testicular disorders," in *Williams Textbook of Endocrinology*, H. M. Kronenberg, M. Melmed, K. S. Polonsky, and P. R. Larsen, Eds., pp. 645–699, Saunders, Philadelphia, Pa, USA, 11th edition, 2008.

[2] M. Shozu, S. Sebastian, K. Takayama et al., "Estrogen excess associated with novel gain-of-function mutations affecting the aromatase gene," *New England Journal of Medicine*, vol. 348, no. 19, pp. 1855–1865, 2003.

[3] M. Demura, R. M. Martin, M. Shozu et al., "Regional rearrangements in chromosome 15q21 cause formation of cryptic promoters for the CYP19 (aromatase) gene," *Human Molecular Genetics*, vol. 16, no. 21, pp. 2529–2541, 2007.

[4] M Fukami, M Shozu, S Soneda et al., "Aromatase excess syndrome: identification of cryptic duplications and deletions leading to gain of function of CYP19A1 and assessment of phenotypic determinants," *The Journal of Clinical Endocrinology & Metabolism*, vol. 96, no. 6, pp. E1035–E1043, 2011.

[5] G. Binder, D. I. Iliev, A. Dufke et al., "Dominant transmission of prepubertal gynecomastia due to serum estrone excess: Hormonal, biochemical, and genetic analysis in a large kindred," *Journal of Clinical Endocrinology and Metabolism*, vol. 90, no. 1, pp. 484–492, 2005.

[6] R. M. Martin, C. J. Lin, M. Y. Nishi et al., "Familial hyperestrogenism in both sexes: clinical, hormonal, and molecular studies of two siblings," *Journal of Clinical Endocrinology and Metabolism*, vol. 88, no. 7, pp. 3027–3034, 2003.

[7] A. Tilpakov, N. Kalintchenko, T. Semitcheva et al., "A potential rearrangement between CYP19 and TRPM7 genes on chromosome 15q21.2 as a cause of aromatase excess syndrome," *The Journal of Clinical Endocrinology & Metabolism*, vol. 90, pp. 4184–4190, 2005.

[8] C. A. Stratakis, A. Vottero, A. Brodie et al., "The aromatase excess syndrome is associated with feminization of both sexes and autosomal dominant transmission of aberrant p450 aromatase gene transcription," *Journal of Clinical Endocrinology and Metabolism*, vol. 83, no. 4, pp. 1348–1357, 1998.

[9] S. Sebastian and S. E. Bulun, "Genetics of endocrine disease: a highly complex organization of the regulatory region of the human CYP19 (Aromatase) gene revealed by the human genome project," *Journal of Clinical Endocrinology and Metabolism*, vol. 86, no. 10, pp. 4600–4602, 2001.

[10] S. E. Bulun, K. Takayama, T. Suzuki, H. Sasano, B. Yilmaz, and S. Sebastian, "Organization of the human aromatase P450 (CYP19) gene," *Seminars in Reproductive Medicine*, vol. 22, no. 1, pp. 5–9, 2004.

[11] M. Demura, S. Reierstad, J. E. Innes, and S. E. Bulun, "Novel promoter I.8 and promoter usage in the CYP19 (aromatase) gene," *Reproductive Sciences*, vol. 15, no. 10, pp. 1044–1053, 2008.

[12] N. Harada, T. Utsumi, and Y. Takagi, "Tissue-specific expression of the human aromatase cytochrome P-450 gene by alternative use of multiple exons 1 and promoters, and switching of tissue-specific exons 1 in carcinogenesis," *Proceedings of the National Academy of Sciences of the United States of America*, vol. 90, no. 23, pp. 11312–11316, 1993.

[13] E. R. Simpson, "Aromatase: biologic relevance of tissue-specific expression," *Seminars in Reproductive Medicine*, vol. 22, no. 1, pp. 11–23, 2004.

[14] E. E. Wallach and C. R. Garcia, "Familial gynecomastia without hypogonadism: a report of three cases in one family," *The Journal of Clinical Endocrinology and Metabolism*, vol. 22, pp. 1201–1206, 1962.

[15] G. D. Berkovitz, A. Guerami, T. R. Brown, P. C. MacDonald, and C. J. Migeon, "Familial gynecomastia with increased extraglandular aromatization of plasma carbon19-steroids," *The Journal of Clinical Investigation*, vol. 75, no. 6, pp. 1763–1769, 1985.

[16] W. Gu, F. Zhang, and J. R. Lupski, "Mechanisms for human genomic rearrangements," *Pathogenetics*, vol. 1, article 4, 2008.

[17] M. B. Yilmaz, A. Wolfe, Y. H. Cheng, C. Glidewell-Kenney, J. L. Jameson, and S. E. Bulun, "Aromatase promoter I.f is regulated by estrogen receptor alpha (ESR1) in mouse hypothalamic neuronal cell lines," *Biology of Reproduction*, vol. 81, no. 5, pp. 956–965, 2009.

[18] J. E. Mercer, D. J. Phillips, and I. J. Clarke, "Short-term regulation of gonadotropin subunit mRNA levels by estrogen: studies in the hypothalamo-pituitary intact and hypothalamo-pituitary disconnected ewe," *Journal of Neuroendocrinology*, vol. 5, no. 5, pp. 591–596, 1993.

[19] D. C. Alexander and W. L. Miller, "Regulation of ovine follicle-stimulating hormone β-chain mRNA by 17β-estradiol in vivo and in vitro," *Journal of Biological Chemistry*, vol. 257, no. 5, pp. 2282–2286, 1982.

[20] T. R. Kumar, Y. Wang, N. Lu, and M. M. Matzuk, "Follicle stimulating hormone is required for ovarian follicle maturation but not male fertility," *Nature Genetics*, vol. 15, no. 2, pp. 201–204, 1997.

PRKAR1A Mutation Affecting cAMP-Mediated G Protein-Coupled Receptor Signaling in a Patient with Acrodysostosis and Hormone Resistance

Keisuke Nagasaki, Tomoko Iida, Hidetoshi Sato, Yohei Ogawa, Toru Kikuchi, Akihiko Saitoh, Tsutomu Ogata, and Maki Fukami

Department of Molecular Endocrinology (K.N., T.O., M.F.), National Research Institute for Child Health and Development, Tokyo 157-8535, Japan; Division of Pediatrics (K.N., H.S., Y.O., T.K., A.S.), Department of Homeostatic Regulation and Development, Niigata University Graduate School of Medical and Dental Sciences, Niigata, 951-8510, Japan; Department of Pediatrics (T.I.), Niigata National Hospital, Niigata, 945-8585, Japan; and Department of Pediatrics (T.O.), Hamamatsu University School of Medicine, Hamamatsu 431-3192, Japan

Context: Acrodysostosis is a rare autosomal dominant disorder characterized by short stature, peculiar facial appearance with nasal hypoplasia, and short metacarpotarsals and phalanges with cone-shaped epiphyses. Recently, mutations of *PRKAR1A* and *PDE4D* downstream of *GNAS* on the cAMP-mediated G protein-coupled receptor (GPCR) signaling cascade have been identified in acrodysostosis with and without hormone resistance, although functional studies have been performed only for p.R368X of *PRKAR1A*.

Objective: Our objective was to report a novel *PRKAR1A* mutation and its functional consequence in a Japanese female patient with acrodysostosis and hormone resistance.

Patient: This patient had acrodysostosis-compatible clinical features such as short stature and brachydactyly and mildly elevated serum PTH and TSH values.

Results: Although no abnormality was detected in *GNAS* and *PDE4D*, a novel *de novo* heterozygous missense mutation (p.T239A) was identified at the cAMP-binding domain A of *PRKAR1A*. Western blot analysis using primary antibodies for the phosphorylated cAMP-responsive element (CRE)-binding protein showed markedly reduced CRE-binding protein phosphorylation in the forskolin-stimulated lymphoblastoid cell lines of this patient. CRE-luciferase reporter assays indicated significantly impaired response of protein kinase A to cAMP in the HEK293 cells expressing the mutant p.T239A protein.

Conclusions: The results indicate that acrodysostosis with hormone resistance is caused by a heterozygous mutation at the cAMP-binding domain A of *PRKAR1A* because of impaired cAMP-mediated GPCR signaling. Because *GNAS*, *PRKAR1A*, and *PDE4D* are involved in the GPCR signal transduction cascade and have some different characters, this would explain the phenotypic similarity and difference in patients with *GNAS*, *PRKAR1A*, and *PDE4D* mutations. (***J Clin Endocrinol Metab* 97: E1808–E1813, 2012**)

Acrodysostosis is a rare autosomal dominant disorder characterized by short stature, peculiar facial appearance with nasal hypoplasia, short metacarpotarsals and phalanges with cone-shaped epiphyses, and variable degrees of mental retardation (1, 2). Recent studies have shown that acrodysostosis is caused by mutations of *PRKAR1A* (protein

ISSN Print 0021-972X ISSN Online 1945-7197
Printed in U.S.A.

doi: 10.1210/jc.2012-1369 Received February 9, 2012. Accepted May 25, 2012.
First Published Online June 20, 2012

Abbreviations: AHO, Albright's hereditary osteodystrophy; CRE, cAMP-responsive element; CREB, CRE-binding; DMR, differentially methylated regions; GNAS, stimulatory G protein α-subunit; GPCR, G protein-coupled receptor; PDE4D, phosphodiesterase 4D, cAMP-specific; PHP-Ia, pseudohypoparathyroidism type Ia; PKA, protein kinase A; PRKAR1A, protein kinase, cAMP-dependent, regulatory type 1, α; RIα, type 1α regulatory subunit.

kinase, cAMP-dependent, regulatory type 1,α) and *PDE4D* (phosphodiesterase 4D, cAMP-specific) involved in the cAMP-mediated G protein-coupled receptor (GPCR) signaling cascade (3–5). *PRKAR1A* consists of 11 exons and encodes type 1α regulatory subunit (RIα) of protein kinase A (PKA) with a dimerization domain, an inhibitory site, and two cAMP-binding domains A and B (6). The PKA holoenzyme is a tetramer consisting of two regulatory subunits and two catalytic subunits, and cooperative binding of two cAMP molecules to each regulatory subunit leads to the dissociation of the catalytic subunits from the regulatory subunits (7). The regulatory subunit-associated catalytic subunits remain inactive, whereas the free catalytic subunits released from the regulatory subunits can phosphorylate a variety of substrate proteins including the cAMP-responsive element (CRE)-binding (CREB) protein (7, 8). It is likely, therefore, that the *PRKAR1A* mutations hinder the cAMP-mediated dissociation of the catalytic subunits from the regulatory subunits, thereby leading to reduced PKA signaling (3). *PDE4D* comprises 15 exons and encodes cAMP-dependent phosphodiesterase 4D (PDE4D) that regulates intracellular cAMP concentrations by converting cAMP to AMP (9). Thus, the *PDE4D* mutations appear to result in desensitization to cAMP because of persistently elevated intracellular cAMP concentrations, thereby affecting the cAMP-mediated GPCR signaling cascade (4). However, functional studies have been performed only for the *PRKAR1A* p.R368X mutation that resides on the last exon and is predicted to escape nonsense-mediated mRNA decay (3), whereas protein modeling analysis argues for the pathological consequences of the remaining *PRKAR1A* and *PDE4D* mutations (4, 5).

Notably, nine of 10 *PRKAR1A* mutation-positive patients and two of seven *PDE4D* mutation-positive patients identified to date exhibit resistance to PTH and/or TSH. Such clinical findings, *i.e.* acrodysostosis plus hormone resistance, overlap with those of pseudohypoparathyroidism type Ia (PHP-Ia), because PHP-Ia is associated with Albright's hereditary osteodystrophy (AHO) reminiscent of acrodysostosis and resistance to several hormones such as PTH and TSH. Indeed, although acrodysostosis and AHO have been classified as different skeletal disorders (2), it is often difficult to distinguish between acrodysostosis and AHO on the basis of clinical and radiological findings (10). Consistent with such phenotypic similarities, PHP-Ia is primarily caused by heterozygous loss-of-function mutations of *GNAS* (the stimulatory G protein α-subunit) (11) that resides in the upstream of *PRKAR1A* and *PDE4D* on the cAMP-mediated GPCR signaling cascade.

Here, we report on a novel *de novo PRKAR1A* mutation and its functional consequence in a patient with acrodysostosis and hormone resistance and discuss phenotypic findings in patients with *PRKAR1A*, *PDE4D*, and *GNAS* mutations.

Patients and Methods

Case report

This Japanese female patient was born to nonconsanguineous parents at 38 wk of gestation. At birth, her length was 46.5 cm (−0.75 SD) and her weight 1.81 kg (−2.8 SD). Neonatal screening tests were normal. Her gross motor milestones were somewhat delayed, with sitting alone without support at 10 months and walking alone at 21 months of age. Her stature remained below −2.0 SD of the mean.

At 3 yr and 10 months of age, she was referred to us because of short stature. Her height was 86.9 cm (−3.1 SD) and her weight 10.6 kg (−2.3 SD). She exhibited round face, nasal hypoplasia, anteverted nostrils, severe brachydactyly of the hands, and mild developmental retardation, and hand roentgenograms showed generalized shortening of the tubular bones with cone shaped epiphyses (Fig. 1A). Brain computerized tomography showed neither sc nor intracranial calcifications. Biochemical and endocrine studies revealed 1) increased serum PTH and plasma cAMP values and normal serum calcium, phosphate, and vitamin D values; 2) decreased urine calcium/creatinine ratio and normal percent tubular reabsorption of phosphate; 3) slightly elevated serum TSH value and normal free T_4 value; 4) age-appropriate serum LH and FSH values; and 5) normal GH response to GHRH stimulation (Table 1). Thus, she was suspected as having acrodysostosis with mild resistance to PTH and TSH.

The parents showed neither brachydactyly nor abnormal endocrine findings (Table 1), although the mother had short stature (144 cm, −2.6 SD).

Molecular and functional studies

We performed 1) direct sequencing for coding exons and their splice sites of *PRKAR1A*, *PDE4D*, and *GNAS*; 2) methylation analysis for four differentially methylated regions (DMR) around *GNAS*; 3) parental testing by microsatellite genotyping; 4) conservation of a substituted amino acid; 5) the forskolin-induced PKA activity of lymphoblastoid cell lines in terms of the phosphorylation status of the CREB protein using Western blot analysis; and 6) forskolin-induced PKA activity using HEK293 cells expressing the wild-type and the mutant proteins. The primers used in this study are shown in Supplemental Table 1, and the detailed methods are described in Supplemental Methods (published on The Endocrine Society's Journals Online web site at http://jcem.endojournals.org).

Results

Analysis of *PRKAR1A*, *PDE4D*, and *GNAS*

No pathological mutation was found for *PDE4D* and *GNAS*, nor was an aberrant methylation pattern detected for the DMR around *GNAS*. By contrast, a novel heterozygous missense mutation (c.715A→G; p.T239A)

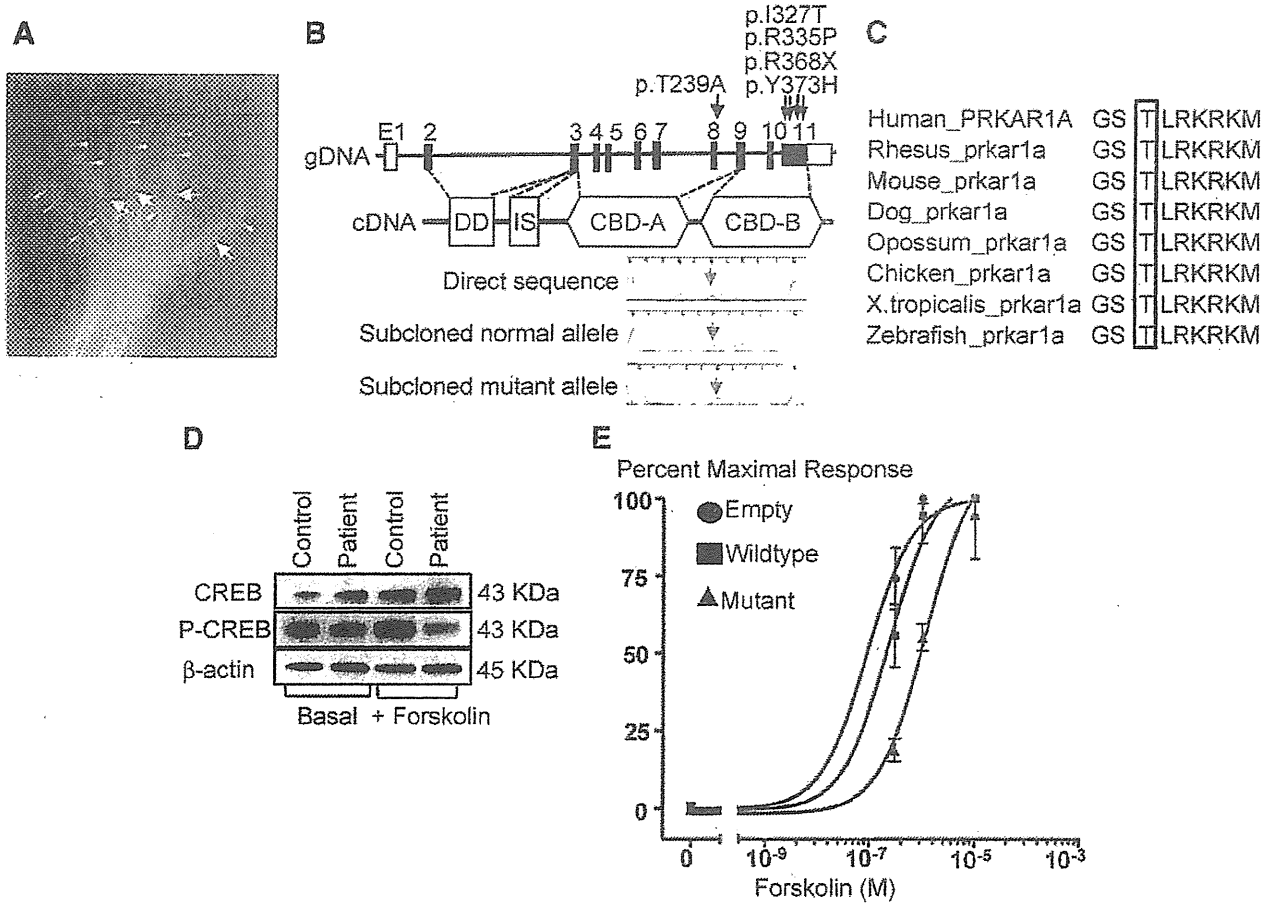

FIG. 1. Representative clinical and experimental findings of this patient. A, Radiograph of the left hand at 3 yr and 10 months of age. Note the shortening of all tubular bones with cone-shaped epiphyses (*arrows*) and early infusions (*arrowheads*). B, The structure of *PRKAR1A* and the position of the mutations identified. The *black and white boxes* on genomic DNA (gDNA) denote the coding regions on exons 2–11 and the untranslated regions, respectively. *PRKAR1A* encodes a dimerization domain (DD), an inhibitory site (IS), and two cAMP-binding domains A and B (CBD-A and -B). A missense mutation (p.T239A) was identified on exon 8 for the cAMP-binding domain A of this patient, whereas the previously described one nonsense and three missense mutations have been found on exon 11 for cAMP-binding domain B (3–5). C, Amino acid sequence of PRKAR1A. Note that the T239 residue is well conserved among species. D, Representative results of Western blot analysis for lymphoblastoid cell lines of the patient and a control subject. The cells were collected before (basal) and after stimulation with 10 μM forskolin. The samples were probed with antibodies for phospho-CREB protein (Ser 133) (P-CREB) and CREB protein, together with those for β-actin used as an internal control. E, Transactivating activities of the wild-type and the mutant PRKAR1A for the CRE-luc reporter. HEK293 cells were transfected with an empty expression vector or with vectors containing either the wild-type PRKAR1A or the p.T239A mutant. Samples were treated with various concentrations of forskolin. The values (percentages to the maximal CRE-luciferase activity) are expressed as the mean ± SE. Curves are fitted with sigmoidal dose-response models. In cells expressing the mutant protein, forskolin induced a concentration-dependent increase in CRE-luciferase activity, yet with a shift to the right in the dose-response curve. The EC_{50} values were significantly higher in the cells expressing the mutant protein than those expressing the wild-type protein ($P < 0.001$). The results are obtained from three independent experiments.

was identified on exon 8 at the cAMP-binding site A of *PRKAR1A* (Fig. 1B). This mutation was absent from her parents and 100 Japanese control subjects.

Parental testing

Microsatellite genotyping data were consistent with paternity as well as maternity of the parents (Supplemental Table 2).

Functional characterization of the mutant *PRKAR1A*

The T239 residue was well conserved among species (Fig. 1C). Protein modeling analysis indicated that the p.T239A resulted in loss of the hydrogen bond between the M236 and the T239 residues and in aberration of the random coils in the mutant PRKAR1A protein, although there was no gross conformational alteration affecting α-helices and β-strands (Supplemental Fig. 1). Western blot analysis indicated obviously reduced forskolin-induced CREB protein phosphorylation in the presence of the apparently normal amount of CREB protein in the lymphoblastoid cell line of this patient (Fig. 1D). Similarly, forskolin-induced PKA activity was significantly lower in the HEK293 cells expressing the mutant PRKAR1A protein than in those expressing the wild-type protein (Fig. 1E).

TABLE 1. Clinical and laboratory data of the patient and her parents

	Patient	Father	Mother[a]
Age (yr)	3 10/12	31	30
Height (cm) (SDS)	**86.9** (−3.1)	177 (+1.1)	**144** (−2.6)
Weight (kg) (SDS)	**10.9** (−2.3)	**89 (+2.5)**	45[b]
Blood			
Intact PTH (pg/ml)	**128** (10–65)	42 (10–65)	23 (10–65)
Calcium (mg/dl)	9.4 (8.5–10.2)	9.4 (8.5–10.2)	9.0 (8.5–10.2)
Phosphate (mg/dl)	5.6 (3.5–5.9)	3.2 (2.4–4.3)	3.6 (2.4–4.3)
25-Hydroxyvitamin D (ng/ml)	26 (7–41)	NA	NA
TSH (mU/liter)	**7.2** (0.5–5.0)	1.7 (0.5–5.0)	1.2 (0.5–5.0)
Free T_4 (ng/ml)	1.2 (0.9–1.6)	1.3 (0.9–1.6)	1.1 (0.9–1.6)
LH (IU/liter)	<0.1 (<0.7)	4.1 (0.8–5.7)	0.17 (1.8–10.2)[c]
FSH (IU/liter)	0.9 (0.6–5.3)	6.6 (2.0–8.3)	0.07 (3.0–14.7)[c]
GH (ng/ml) stimulated[d]	19.5 (>9)	NA	NA
cAMP (pmol/ml)	**39.6** (6.4–20.8)	NA	NA
Urine			
Calcium/creatinine ratio	**0.04** (0.13–0.25)	NA	NA
% TRP	91 (81.3–93.3)	NA	NA

The values in *parentheses* indicate the SD score (SDS) for heights and weights and the age-and sex-matched reference blood and urine hormone and laboratory data. The conversion factors to the SI unit are as follows: intact PTH, 1.0 (nanograms per liter); serum calcium, 0.25 (millimoles per liter); serum phosphate, 0.3229 (millimoles per liter); 25-hydroxyvitamin D, 2.496 (nanomoles per liter); free T_4, 12.9 (picomoles per liter); GH, 1.0 (micrograms per liter); and cAMP, 1.0 (nanomoles per liter). Hormone values have been evaluated by the age- and sex-matched Japanese reference data; abnormal data are in *bold*. NA, Not available; TRP, tubular reabsorption of phosphate.

[a] During the second trimester of pregnancy.

[b] Not assessed because of pregnancy.

[c] Low LH/FSH values are consistent with pregnant status of the mother (18).

[d] Blood sampling during the provocation tests were done at 0, 30, 60, 90, and 120 min after GHRH stimulation (1 μg/kg).

Discussion

We identified a novel *de novo* heterozygous *PRKAR1A* mutation in a patient with acrodysostosis and mild resistance to PTH and TSH. In this regard, several findings are noteworthy. First, although the phenotypic findings of this patient are similar to those of PHP-Ia, the severe skeletal lesion would be regarded as acrodysostosis rather than AHO. Consistent with this, a mutation was identified in *PRKAR1A* rather than *GNAS*. Second, the p.T239A was present at the cAMP-binding domain A, in contrast to the previously reported *PRKAR1A* mutations that were invariably located at the cAMP-binding domain B (3–5). In this regard, because cAMP binds first to the binding domain B and then to the binding domain A, it has been suggested that the binding domain B acts as the gatekeeper of the PKA activation, and that the binding domain A is relatively inaccessible to cAMP (8). Despite such a hierarchical phenomenon, this study indicates that mutations at the cAMP-binding domains A and B lead to a similar clinical phenotype. Third, functional analyses showed obviously reduced PKA signaling of the mutant PRKAR1A protein. Thus, the p.T239A mutation appears to impair the dissociation of the catalytic subunits from the RIα regulatory subunits, thereby leading to the reduced GPCR signaling, as has been stated by the functional studies for the p.R368X mutation (3). Although the underlying factors remains to be elucidated, loss of the hydrogen bond and aberration of the random coils in the mutant PRKAR1A protein may be relevant to this functional alteration.

To date, *GNAS*, *PRKAR1A*, and *PDE4D* mutations have been identified in patients with overlapping skeletal and endocrine phenotypes (3–5). It appears, however, that *GNAS* abnormalities usually lead to relatively mild skeletal phenotype and clinically discernible hormone resistance, whereas *PRKAR1A* and *PDE4D* mutations usually result in relatively severe skeletal lesion and mild or absent hormone resistance. In this regard, it is predicted in patients with maternally derived *GNAS* mutations that normally functioning *GNAS* is absent from several tissues including renal proximal tubules where *GNAS* is paternally imprinted and is present in a single copy in other tissues including skeletal tissues where *GNAS* is biparentally expressed (11, 12). By contrast, it is likely in patients with *PRKAR1A* and *PDE4D* mutations that normally functioning *PRKAR1A* and *PDE4D* are present in a single copy in all the tissues because of the absence of DMR around these genes (13). Such a difference in the functional gene dosage in several *GNAS*-imprinted tissues may more or less be relevant to the prevalent hormone resistance in *GNAS* mutations. Furthermore, because there are four genes encoding the regulatory subunits of PKA (RIa, RIb,

RIIa, and RIIb) and three genes encoding the catalytic subunits (14), such redundancy would also be related to the apparently mild hormone resistance in *PRKAR1A* mutations. However, these factors are unlikely to account for the apparently severe skeletal lesion in *PRKAR1A* and *PDE4D* mutations. Furthermore, although aberrant signaling via PTHrP receptor belonging to the GPCR families may play an important role in the development of skeletal lesions in *PRKAR1A* mutations, this perturbation is also relevant to the occurrence of skeletal lesions in *GNAS* abnormalities (15). Thus, there may be a hitherto unknown factor involved in the development of severe skeletal phenotype in *PRKAR1A* and *PDE4D* mutations. Notably, hormone resistance is apparently infrequent in acrodysostosis (2). It remains to be clarified whether acrodysostosis with and without hormone resistance may represent genetically heterogeneous conditions, and whether hormone resistance may have been overlooked or remained at a subclinical level in a certain fraction of patients with *PRKAR1A* and *PDE4D* mutations.

For *PRKAR1A*, more than 100 different mutations have been identified in Carney complex with multiple neoplasias and lentiginosis (16). Because most mutations reported in Carney complex are frameshift, nonsense, and splice mutations that are predicted to undergo nonsense-mediated mRNA decay and cause *PRKAR1A* haploinsufficiency, they would result in the increased amount of the free-lying intracellular catalytic subunits, leading to excessive PKA signaling in target tissues (16, 17). Furthermore, other types of mutations have also been identified in Carney complex, such as missense mutations at the cAMP-binding domain A (*e.g.* p.D183Y and p.A213D) and an in-frame deletion of 53 amino acids from the binding domain A (c.708 + 1 g→t) (16). Thus, in conjunction with the results of this study, we presume that *PRKAR1A* mutations can cause a mirror image of disorders in terms of the PKA activity, *i.e.* Carney complex resulting from defective association between the regulatory and the catalytic subunits and acrodysostosis with hormone resistance ascribed to impaired dissociation between the two subunits.

In summary, we identified a heterozygous *PRKAR1A* mutation affecting cAMP-mediated GPCR signaling in a patient with acrodysostosis with hormone resistance. Additional studies will permit a better clarification of the underlying causes in acrodysostosis with and without hormone resistance.

Acknowledgments

We thank Professor N. Matsuura (Seitoku University) and Dr. S. Narumi (Keio University School of Medicine) for fruitful discussion. We are grateful to Drs. N. Katsumata and S. Takada and Ms. A. Nagashima, T. Tanji, E. Suzuki, and I. Kobayashi (National Research Institute for Child Health and Development) for their technical assistance.

Address all correspondence and requests for reprints to: Dr. Tsutomu Ogata, Department of Pediatrics, Hamamatsu University School of Medicine, Hamamatsu 431-3192, Japan. E-mail: tomogata@hama-med.ac.jp; or Dr. Maki Fukami, Department of Molecular Endocrinology, National Research Institute for Child Health and Development, Tokyo 157-8535, Japan. E-mail: mfukami@nch.go.jp.

This work was supported by the Grant-in-Aid for Scientific Research on Innovative Areas (22132004) from the Ministry of Education, Culture, Sports, Science, and Technology; by the Grant-in-Aid for Scientific Research (B) (23390249) from the Japan Society for the Promotion of Science; and by grants from the Foundation for Growth Science, from the National Center for Child Health and Development (23A-1), and from the Ministry of Health, Labor, and Welfare.

Disclosure Summary: The authors declare no conflict of interest.

References

1. **Wilson LC, Oude Luttikhuis ME, Baraitser M, Kingston HM, Trembath RC** 1997 Normal erythrocyte membrane Gsα bioactivity in two unrelated patients with acrodysostosis. J Med Genet 34:133–136
2. **Graham Jr JM, Krakow D, Tolo VT, Smith AK, Lachman RS** 2001 Radiographic findings and Gs-α bioactivity studies and mutation screening in acrodysostosis indicate a different etiology from pseudohypoparathyroidism. Pediatr Radiol 31:2–9
3. **Linglart A, Menguy C, Couvineau A, Auzan C, Gunes Y, Cancel M, Motte E, Pinto G, Chanson P, Bougnères P, Clauser E, Silve C** 2011 Recurrent PRKAR1A mutation in acrodysostosis with hormone resistance. N Engl J Med 364:2218–2226
4. **Lee H, Graham Jr JM, Rimoin DL, Lachman RS, Krejci P, Tompson SW, Nelson SF, Krakow D, Cohn DH** 2012 Exome sequencing identifies PDE4D mutations in acrodysostosis. Am J Hum Genet 90:746–751
5. **Michot C, Le Goff C, Goldenberg A, Abhyankar A, Klein C, Kinning E, Guerrot AM, Flahaut P, Duncombe A, Baujat G, Lyonnet S, Thalassinos C, Nitschke P, Casanova JL, Le Merrer M, Munnich A, Cormier-Daire V** 2012 Exome sequencing identifies PDE4D mutations as another cause of acrodysostosis. Am J Hum Genet 90:740–745
6. **Scott JD** 1991 Cyclic nucleotide-dependent protein kinases. Pharmacol Ther 50:123–145
7. **Taskén K, Skålhegg BS, Solberg R, Andersson KB, Taylor SS, Lea T, Blomhoff HK, Jahnsen T, Hansson V** 1993 Novel isozymes of cAMP-dependent protein kinase exist in human cells due to formation of RIα-RIβ heterodimeric complexes. J Biol Chem 268:21276–21283
8. **Kim C, Xuong NH, Taylor SS** 2005 Crystal structure of a complex between the catalytic and regulatory (RIα) subunits of PKA. Science 307:690–696
9. **Verghese MW, McConnell RT, Lenhard JM, Hamacher L, Jin SL** 1995 Regulation of distinct cyclic AMP-specific phosphodiesterase (phosphodiesterase type 4) isozymes in human monocytic cells. Mol Pharmacol 47:1164–1171
10. **Ablow RC, Hsia YE, Brandt IK** 1977 Acrodysostosis coinciding with pseudohypoparathyroidism and pseudo-pseudohypoparathyroidism. AJR Am J Roentgenol 128:95–99